Specific Synthesis and Reaction of Hetero- and Homobridged Diruthenium Carbonyl Complexes Containing One or Two μ-Azolato Bridges

Kom-Bei Shiu,* Wei-Ming Lee, and Chen-Lan Wang

Department of Chemistry, National Cheng Kung University, Tainan, Taiwan 701, Republic of China

Sue-Lein Wang and Fen-Ling Liao

Department of Chemistry, National Tsing Hua University, Hsinchu, Taiwan 300, Republic of China

Ju-Chun Wang and Lin-Shu Liou

Department of Chemistry, Soochow University, Taipei, Taiwan 111, Republic of China

Shie-Ming Peng and Gene-Hsiang Lee

Department of Chemistry, National Taiwan University, Taipei, Taiwan 106, Republic of China

Michael Y. Chiang

Department of Chemistry, National Sun Yat-Sen University, Kaohsiung, Taiwan 804, Republic of China

Received February 5, 1996[⊗]

Diruthenium(I) carbonyl complexes with either hetero- or homobridges, $[Ru_2(\mu\text{-}Pz)_2(CO)_4(HPz)_2]$ (**1**), $[Ru_2(\mu\text{-}Pz')(\mu\text{-}O_2CMe)(CO)_4(HPz')_2]$ (**2**), and $[Ru_2(\mu\text{-}Pz')_2(CO)_4(HPz')_2]$ (**3**), can be prepared specifically. These complexes reacted with either nucleophiles or electrophiles to produce selectively only one product. The terminal azole groups, pyrazole (HPz) or 3,5-dimethylpyrazole (HPz′), of **1**−**3** are easily replaced by the phosphine ligands to give $[Ru_2(\mu\text{-}Pz)_2(CO)_4(PPh_3)_2]$ (**4**), $[Ru_2(\mu\text{-}Pz')(\mu\text{-}O_2CMe)(CO)_4(PPh_3)_2]$ (**5**), $[Ru_2(\mu\text{-}Pz')_2(CO)_4(PPh_3)_2]$ (**6**), and $[Ru_2(\mu\text{-}Pz)_2(CO)_4(\eta^1\text{-dppm})_2]$ (**7**). The μ-acetato bridge is more fragile than the μ-azolato bridge, and only the former bridge of **5** can be replaced by Pz^- and SR^- to afford $[Ru_2(\mu\text{-}Pz')(\mu\text{-}Pz)(CO)_4(PPh_3)_2]$ (**8**) and $[Ru_2(\mu\text{-}Pz')(\mu\text{-}SR)(CO)_4(PPh_3)_2]$ (R = Ph (**9**), ^{t}Bu (**10**)). Heating the mixture of **3** with dppm in THF gave a product retaining all the μ-azolato bridges but losing two carbonyls, $[Ru_2(\mu\text{-}Pz')_2(CO)_2(\mu_1,\eta^2\text{-dppm})_2]$ (**11**), whereas a similar reaction between **1**−**3** and nitrogen-bidentate ligands gave products retaining all four carbonyls but only one μ-azolato bridge, $[Ru_2(\mu\text{-}L)(\mu\text{-}CO)_2(CO)_2(\mu_1,\eta^2\text{-}(N{-}N))_2]^+$ (L = Pz, N−N = bpy ([**12**]$^+$), phen ([**13**]$^+$); L = Pz′, N−N = bpy ([**14**]$^+$), phen ([**15**]$^+$)). The electrophilic addition of **4** with I_2 produced $[Ru_2(\mu\text{-}Pz)_2(\mu\text{-}I)(CO)_4(PPh_3)_2][I_3]$ (**16**). The X-ray structure of this product confirms the cleavage of the Ru−Ru bond rather than the μ-azolato bridges. However, the μ-azolato and -acetato bridges, as well as the terminal azole groups, of **1**−**6** can be easily removed by an electrophilc reagent such as $Et_3O^+BF_4^-$ in the presence of MeCN to give $[Ru_2(CO)_4(MeCN)_6][BF_4]_2$ and $[Ru_2(CO)_4(MeCN)_4(PPh_3)_2][BF_4]_2$.

Introduction

The coordination chemistry of the dirhodium and -iridium complexes has been well studied recently. Particularly, those containing the μ-azolato bridging group are under intensive investigations, due to the ability of the apparently strong μ-azolato bridge enabling to straddle an unusual range of intermetallic separations to hold two adjacent metal centers in chemically extremely stable configurations.[1] In view of the rarely studied coordination chemistry of the diruthenium complexes with the μ-azolato bridge,[2] and the significance of the diruthenium(I) carbonyl complexes in being either involved as the active intermediates in homogeneously catalyzed reactions or catalytic precursors for the carbonylation of amines, the hydrogenation of carboxylic acids, and the addition of acetic acid to alkynes,[3] we decided to explore the synthesis and reactivity some diruthenium(I) carbonyl complexes containing the μ-azolato linkage.

In this paper, we present the following new information: (1) a convenient approach to prepare *specifically* both hetero- and homobridged diruthenium carbonyl complexes with one or two μ-azolato linkages, (2) the *selective* nucleophilic and electrophilic reactions of these complexes to give only one type of product, (3) the X-ray

[⊗] Abstract published in *Advance ACS Abstracts,* May 15, 1996.

S0276-7333(96)00070-2 CCC: $12.00

structures of eight representative reaction products, and (4) the novel propensity of the μ-azolato linkage, especially the cleavable feature first found in the dimetal system.

Results and Discussion

Synthesis. Although complexes $[Ru_2(\mu\text{-L})_2(CO)_6]$ (HL = pyrazole (HPz), 3,5-dimethylpyrazole (HPz′)) were previously described to be important precursors to several other ruthenium derivatives, the synthetic approaches used suffer either a low yield[2a,e] or a tedious procedure.[2c] As demonstrated below, new dinuclear species in the types of $[Ru_2(\mu\text{-L})_2(CO)_4(HL)_2]$ and $[Ru_2(\mu\text{-Pz}')(\mu\text{-O}_2\text{CMe})(CO)_4(HPz')_2]$ can be obtained specifically in satisfactory yield and employed as better precursors to a variety of other Ru(I) and Ru(II) derivatives. Importantly, all the conversions appear to follow selective pathways.

In the presence of Et_3N, *catena*-$[Ru(O_2CMe)(CO)_2]$ reacted with excess HPz or HPz′ in EtOH gave only one diruthenium derivative with either homo- or heterobridges, $[Ru_2(\mu\text{-Pz})_2(CO)_4(HPz)_2]$ (**1**) and $[Ru_2(\mu\text{-Pz}')(\mu\text{-O}_2\text{CMe})(CO)_4(HPz')_2]$ (**2**), respectively. The homobridged compounds **1** can be obtained alternatively from the reaction of $[Ru_2(CO)_4(MeCN)_6][BF_4]_2$ with HPz/Et_3N and H_2O. Complex $[Ru_2(\mu\text{-Pz}')_2(CO)_4(HPz')_2]$ (**3**) can be obtained likewise. The reactions involve obviously first the substitution of MeCN in $[Ru_2(CO)_4(MeCN)_6][BF_4]_2$ with a better σ-donor, L^-, via HL/Et_3N to give $[Ru_2(\mu,\eta^2\text{-L})_2(CO)_4(\eta^1\text{-L})]^{2-}$ and then protonation with H_2O to give **1** and **3** (Scheme 1). The specific formation of **2** rather than a mixture of **2** and **3** reflects probably that the nucleophilic substitution is stepwise and the steric hindrance of μ-Pz′ in **2** may inhibit a subsequent replacement of the remaining μ-acetato group by a second Pz'^-.

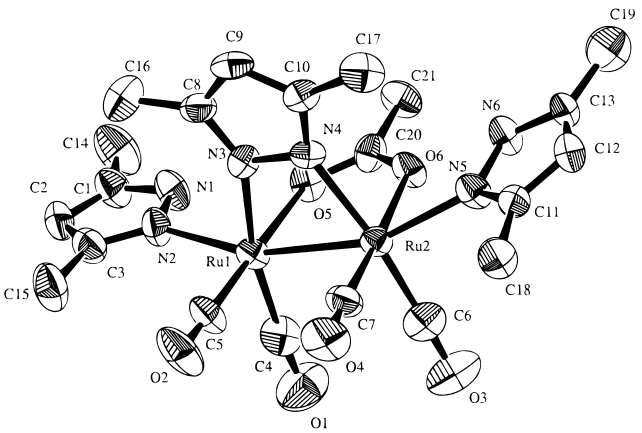

Figure 1. ORTEP plot of **2** with 50% thermal ellipsoids.

Scheme 1

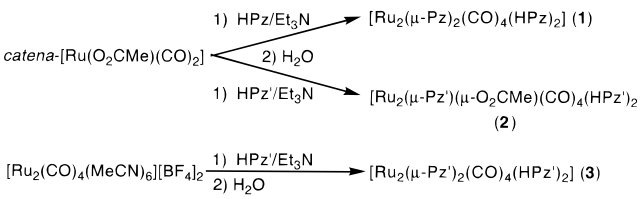

Compound **2** was structurally characterized (Figure 1). The heterobridged feature and the two HPz′ groups ligated to Ru at the axial sites were confirmed. The Ru−Ru distance of 2.682(1) Å in **2** (Table 1) is significantly shorter than that of 2.705(2) Å in $[Ru_2(\eta^2\text{-Pz}')_2(CO)_6]$.[2a,e] The longer distance may be due to a combination of both electronic and steric factors. The higher *trans* influence of the axial carbonyls in this compound, compared with that of the axial HPz′ groups in **2**, and the larger nonbonded interactions between two bulky μ-Pz′ groups and other groups in $[Ru_2(\eta^2\text{-Pz}')_2(CO)_6]$, compared with those between one such μ-Pz′ group and other groups in **2**, may contribute to the Ru−Ru elongation.

Reactions with Nucleophiles. The two axial groups in either $[Ru_2(\eta^2\text{-L})_2(CO)_6]$[2e] or $[Ru_2(CO)_4(MeCN)_6]^{2+}$ [4a] were previously reported to be substitution labile. Complexes **1**−**3** behave similarly. The two axial HL groups of **1**−**3** are easily replaced by phosphine groups to give $[Ru_2(\mu\text{-Pz})_2(CO)_4(PPh_3)_2]$ (**4**), $[Ru_2(\mu\text{-Pz}')(\mu\text{-O}_2\text{CMe})(CO)_4(PPh_3)_2]$ (**5**), $[Ru_2(\mu\text{-Pz}')_2(CO)_4(PPh_3)_2]$ (**6**), and $[Ru_2(\mu\text{-Pz})_2(CO)_4(\eta^1\text{-dppm})_2]$ (**7**) (Scheme 2) with **5** structurally characterized to confirm the heterobridged feature (Figure 2). The Ru−Ru distance increases from 2.682(1) Å in **2** to 2.7261(9) Å in **5**, apparently due to the increased nonbonded interactions between the bulkier PPh_3 groups and other groups in the molecule.

(1) (a) Uson, R.; Oro, L. A.; Ciriano, M. A.; Pinillos, M. T. *J. Organomet. Chem.* **1981**, *205*, 247. (b) Beveridge, K. A.; Bushnell, G. W.; Dixon, K. R.; Eadie, D. T.; Stobart, S. R.; Atwood, J. L.; Zaworotko, M. J. *J. Am. Chem. Soc.* **1982**, *104*, 920. (c) Coleman, A. W.; Eadie, D. T.; Stobart, S. R.; Zaworotko, M. J.; Atwood, J. L. *J. Am. Chem. Soc.* **1982**, *104*, 922. (d) Bushnell, G. W.; Fjeldsted, O. K.; Stobart, S. R.; Zaworotko, M. J. *J. Chem. Soc., Chem. Commun.* **1983**, 580. (e) Beveridge, K. A.; Bushnell, G. W.; Stobart, S. R.; Atwood, J. L.; Zaworotko, M. J. *Organometallics*, **1983**, *2*, 1447. (f) Bushnell, G. W.; Stobart, S. R.; Vefghi, R.; Zaworotko, M. J. *J. Chem. Soc., Chem. Commun.* **1984**, 282. (g) Atwood, J. L.; Beveridge, K. A.; Bushnell, G. W.; Dixon, K. R.; Eadie, D. T.; Stobart, S. R.; Zaworotko, M. J. *Inorg. Chem.* **1984**, *23*, 4050. (h) Bushnell, G. W.; Fjeldsted, D. O. K.; Stobart, S. R.; Zaworotko, M. J.; Knox, S. A. R.; Macpherson, K. A. *Organometallics* **1985**, *4*, 1107. (i) Bushnell, G. W.; Decker, M. J.; Eadie, D. T.; Stobart, S. R.; Vefghi, R.; Atwood, J. L.; Zaworotko, M. J. *Organometallics* **1985**, *4*, 2106. (j) Claver, C.; Kalck, P.; Ridmy, M.; Thorez, A.; Oro, L. O.; Pinillos, M. T.; Apreda, M. C.; Cano, F. H.; Foces-Foces, C. *J. Chem. Soc., Dalton Trans.* **1988**, 1523. (k) Caromna, D.; Oro, L. O.; Perez, P. L.; Tiripicchio, A.; Tiripicchio-Camellini, M. *J. Chem. Soc., Dalton Trans.* **1989**, 1427. (l) Pinillos, M. T.; Elduque, A.; Oro, L. A. *Inorg. Chim. Acta* **1990**, *178*, 179. (m) Pinillos, M. T.; Elduque, A.; Oro, L. A.; Lahoz, F. J.; Bonati, F.; Tiripicchio, A.; Tiripicchio-Camellini, M. *J. Chem. Soc., Dalton Trans.* **1990**, 989. (n) Pinillos, M. T.; Elduque, A.; Lopez, J. A.; Lahoz, F. J.; Oro, L. A. *J. Chem. Soc., Dalton Trans.* **1991**, 1391. (o) Carmona, D.; Ferrer, J.; Lahoz, F. J.; Oro, L. A.; Reyes, J.; Esteban, M. *J. Chem. Soc., Dalton Trans.* **1991**, 2811. (p) Carmona, D.; Ferrer, J.; Mendoza, A.; Lahoz, F. J.; Reyes, J.; Oro, L. A. *Angew. Chem., Int. Ed. Engl.* **1991**, *30*, 1171. (q) Pinillos, M. T.; Elduque, A.; Oro, L. A. *Polyhedron* **1992**, *11*, 1007. (r) Ciriano, M. A.; Tena, M. A.; Oro, L. A. *J. Chem. Soc., Dalton Trans.* **1992**, 2123. (s) Pinillos, M. T.; Elduque, A.; Lopez, J. A.; Lahoz, F. J.; Oro, L. A.; Mann, B. E. *J. Chem. Soc., Dalton Trans.* **1992**, 2389. (t) Tejel, C.; Ciriano, M. A.; Oro, L. A.; Tiripicchio, A.; Ugozzoli, F. *Organometallics* **1994**, *13*, 4153.

(2) (a) Cabeza, J. A.; Landazuri, C.; Oro, L. A.; Tiripicchio, A.; Tiripicchio-Camellini, M. *J. Organomet. Chem.* **1987**, *322*, C16. (b) Sherlock, S. J.; Cowie, M.; Singleton, E.; Steyn, M. M. d. V. *J. Organomet. Chem.* **1989**, *361*, 353. (c) Neumann, F.; Süss-Fink, G. *J. Organomet. Chem.* **1989**, *367*, 175. (d) Neumann, F.; Stoeckli-Evans, H.; Süss-Fink, G. *J. Organomet. Chem.* **1989**, *379*, 151. (e) Cabeza, J. A.; Landazuri, C.; Oro, L. A.; Belletti, D.; Tiripicchio, A.; Tiripicchio-Camellini, M. *J. Chem. Soc., Dalton Trans.* **1989**, 1093.

(3) (a) Bianchi, M.; Menchi, G.; Francalanci, F.; Piacenti, F.; Matteoli, U.; Frediani, P. *J. Organomet. Chem.* **1980**, *188*, 109. (b) Bianchi, M.; Iani, P. F.; Matteoli, U.; Menchi, G.; Piacenti, F.; Petrucci, G. *J. Organomet. Chem.* **1983,** *259*, 207. (c) Suss-Fink, G.; Hermann, G.; Morys, P.; Ellermann, J.; Veit, A. *J. Organomet. Chem.* **1985**, *284*, 263. (d) Matteoli, U.; Menchi, G.; Frediani, P.; Bianchi, M.; Piacenti, F. *J. Organomet. Chem.* **1985**, *285*, 281. (e) Kalck, P.; Sianti, M.; Jenck, J.; Peyrille, B.; Peres, Y. *J. Mol. Catal.* **1991**, *67*, 19. (f) Frediani, P.; Bianchi, M.; Salvini, A.; Guarducci, R.; Carluccio, L. C.; Piacenti, F. *J. Organomet. Chem.* **1995**, *498*, 187.

(4) (a) Klemperer, W. G.; Zhong, B. *Inorg. Chem.* **1993**, *32*, 5821. (b) Shiu, K.-B.; Li, C.-H.; Chan, T.-J.; Peng, S.-M.; Cheng, M.-C.; Wang, S.-L.; Liao, F.-L.; Chiang, M. Y. *Organometallics* **1995**, *14*, 524.

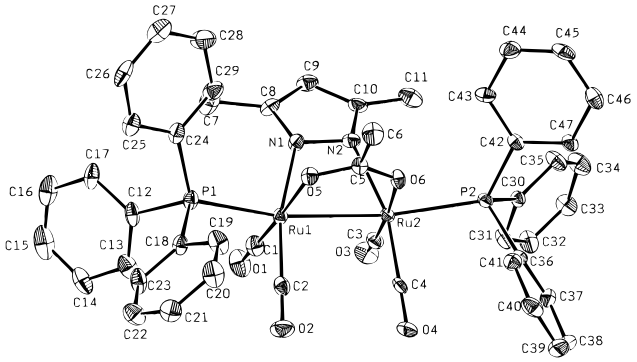

Figure 2. ORTEP plot of **5** with 50% probability ellipsoids.

Scheme 2

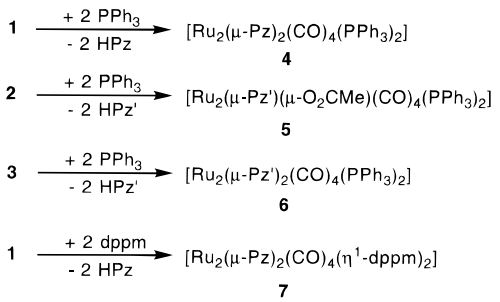

Scheme 3

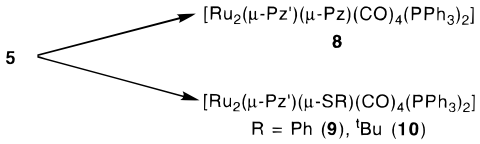

The $^{31}P\{^1H\}$ NMR spectrum of **7**, like that of $[Ru_2(\mu\text{-}O_2CMe)_2(CO)_4(\eta^1\text{-dppm})_2]$,[5] appears as two sets of multiplets at δ 12.12 and −26.18 ppm consistent with an AA′XX′ spin system. The structure of **7** is hence believed to be similar to that of **5**.

The μ-acetato bridge, rather than the μ-Pz′ bridge, in **5** can be replaced further by any smaller or stronger anionic σ-donor, like Pz^- or thiolate anion, to give $[Ru_2(\mu\text{-}Pz')(\mu\text{-}Pz)(CO)_4(PPh_3)_2]$ (**8**) and $[Ru_2(\mu\text{-}Pz')(\mu\text{-}SR)(CO)_4(PPh_3)_2]$ (R = Ph (**9**), ^{t}Bu (**10**)) (Scheme 3), respectively. The $^{31}P\{^1H\}$ NMR spectrum of **10** appears as two doublets indicating probably the asymmetric orientation of either two PPh_3 groups and/or the thiolate bridge with respect to the Ru−Ru bond. **10** may be rigid in solution at room temperature on the NMR time scale. The single-crystal structure of **10** was thus carried out (Figure 3a). It reveals two asymmetrical PPh_3 groups (Figure 3b) with the P(2) group at the axial site and the P(1) group at the equatorial site, probably alleviating the repulsive nonbonded interactions if both groups are at the axial sites. The Ru−Ru distance is 2.7469(5) Å.

The reaction product between $[Ru_2(\mu\text{-}Pz')_2(CO)_6]$ and excess dppm was previously reported by Süss-Fink's group to be $[Ru_2(\mu\text{-}Pz')_2(CO)_4(\eta^1\text{-dppm})_2]$, a formula similar to **7**, but an unusal structure was suggested to have two η^1-dppm and one CO groups at one Ru atom and three CO groups at the other metal atom, probably on the basis of a typical AA′XX′ spin system observed in a $^{31}P\{^1H\}$ NMR spectrum.[2d] However, such a suggestion was questioned, on the basis of our findings that the μ-Pz′ linkage is rather strong and resistant even with respect to a strong nucleophile such as a thiolate anion and that the axial groups in $[Ru_2(\eta^2\text{-L})_2(CO)_6]$, $[Ru_2(CO)_4(MeCN)_6]^{2+}$, or **1**−**3** are substitution labile. In order to obtain a clear-cut conclusion, we attempted a similar substitution reaction by following their reaction condition, *i.e.*, by heating a mixture of **3** and excess dppm in THF for more than 24 h. The compound we obtained shows very similar IR and ^{1}H-NMR spectral data to those reported by Süss-Fink's group. It also exhibits two multiplets consistent with an AA′XX′ spin system at δ 11.41 and −30.26, but these two values differ about 3.6−4.0 ppm from those reported. Further, the elemental analysis results clearly indicate that the compound should not be formulated as $[Ru_2(Pz')_2(CO)_4(dppm)_2]$ but $[Ru_2(Pz')_2(CO)_2(dppm)_2]$ (**11**) with only two, rather than four, carbonyls suggested. The crystal structure of **11** was hence determined to support this formulation. As shown in the simplified ORTEP plot of **11** (Figure 4), each Ru atom of **11** has one chelate dppm and one CO. The two carbonyls, C(1)O(1) and C(2)O(2), are in a gauche conformation with the torsion angle ∠C(1)−Ru(1)−Ru(2)−C(2) = 85.9°. Obviously the bidentate ligand dppm can replace only the axial HPz′ and carbonyl groups rather than cleave one or two apparently strong μ-Pz′ linkages in **3** (Scheme 4).

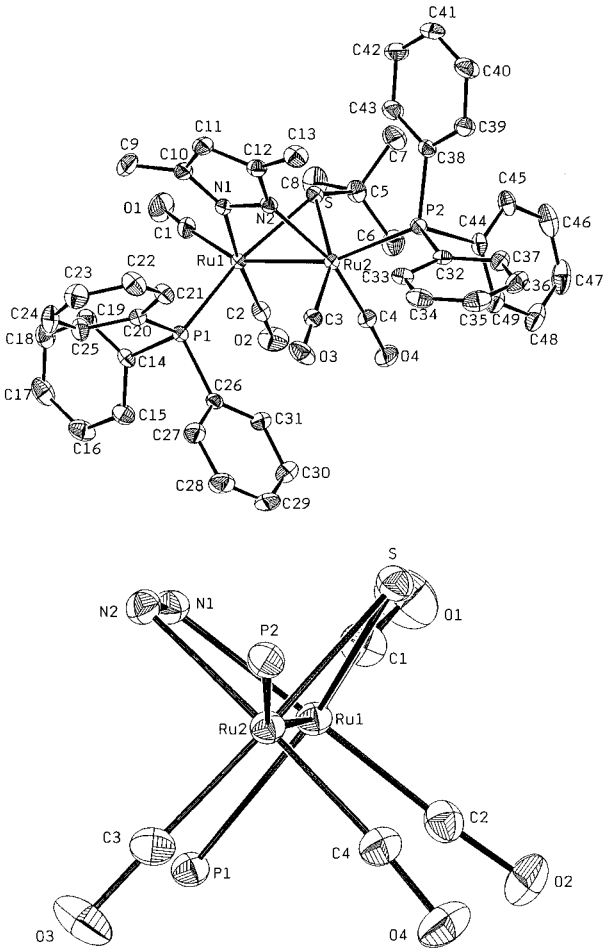

Figure 3. (a) Top: ORTEP plot of **10** with 50% thermal ellipsoids. (b) Bottom: ORTEP plot of **10** along the Ru−Ru axis with phenyl and *tert*-butyl groups omitted.

(5) Sherlock, S. J.; Cowie, M.; Singleton, E.; Steyn, M. M. d. V. *Organometallics* **1988**, *7*, 1663.

Table 1. Selected Bond Lengths (Å) and Angles (deg)

Bond Lengths for **2**

Ru(1)−Ru(2)	2.682(1)	Ru(2)−O(6)	2.170(5)	Ru(1)−N(2)	2.261(7)	C(4)−O(1)	1.17(1)
Ru(1)−N(3)	2.111(7)	C(5)−O(2)	1.135(10)	Ru(1)−C(5)	1.846(10)	C(6)−O(3)	1.160(10)
Ru(1)−C(4)	1.82(1)	C(7)−O(4)	1.155(10)	Ru(1)−O(5)	2.170(6)	C(20)−O(5)	1.278(10)
Ru(2)−N(4)	2.103(7)	C(20)−O(6)	1.252(10)	Ru(2)−N(5)	2.213(7)	N(1)−N(2)	1.362(9)
Ru(2)−C(6)	1.839(10)	N(3)−N(4)	1.376(8)	Ru(2)−C(7)	1.850(10)	N(5)−N(6)	1.341(9)

Bond Angles for **2**

Ru(2)−Ru(1)−N(2)	162.2(2)	O(6)−Ru(2)−C(7)	178.1(3)	Ru(1)−Ru(2)−N(5)	160.0(2)	C(7)−Ru(2)−C(6)	88.1(4)
Ru(2)−Ru(1)−O(5)	84.3(2)	C(6)−Ru(2)−N(4)	169.5(3)	Ru(1)−Ru(2)−O(6)	83.7(1)	Ru(1)−C(4)−O(1)	176.5(9)
O(5)−C(20)−O(6)	123.6(8)	Ru(1)−C(5)−O(2)	179.0(8)	O(5)−Ru(1)−C(5)	178.6(3)	Ru(2)−C(6)−O(3)	178.3(9)
C(5)−Ru(1)−C(4)	92.1(3)	Ru(2)−C(7)−O(4)	178.9(9)	C(4)−Ru(1)−N(3)	167.9(3)		

Bond Lengths for **5**

Ru(1)−Ru(2)	2.7261(9)	Ru(2)−O(6)	2.136(5)	Ru(1)−C(1)	1.834(9)	C(5)−O(5)	1.265(9)
Ru(1)−N(1)	2.129(6)	C(5)−O(6)	1.246(8)	Ru(1)−O(5)	2.142(5)	C(1)−O(1)	1.142(11)
Ru(1)−C(2)	1.871(8)	C(2)−O(2)	1.134(9)	Ru(2)−N(2)	2.127(6)	C(3)−O(3)	1.147(10)
Ru(2)−P(2)	2.4324(21)	C(4)−O(4)	1.140(9)	Ru(2)−C(4)	1.865(7)	N(1)−N(2)	1.379(8)
Ru(2)−C(3)	1.828(8)	Ru(1)−P(1)	2.4357(21)				

Bond Angles for **5**

Ru(2)−Ru(1)−P(1)	166.35(7)	O(6)−Ru(2)−C(3)	174.8(3)	Ru(1)−Ru(2)−P(2)	167.04(6)	C(3)−Ru(2)−C(4)	92.4(3)
Ru(1)−Ru(2)−O(6)	83.66(13)	C(4)−Ru(2)−N(2)	164.8(3)	Ru(2)−Ru(1)−O(5)	82.94(13)	Ru(1)−C(1)−O(1)	178.8(7)
O(5)−C(5)−O(6)	125.1(7)	Ru(1)−C(2)−O(2)	179.2(8)	O(5)−Ru(1)−C(1)	176.0(3)	Ru(2)−C(3)−O(3)	175.8(7)
C(1)−Ru(1)−C(2)	89.8(4)	Ru(2)−C(4)−O(4)	177.7(8)	C(2)−Ru(1)−N(1)	166.4(3)		

Bond Lengths for **10**

Ru(1)−Ru(2)	2.7469(5)	Ru(2)−N(2)	2.153(3)	Ru(1)−P(1)	2.3735(10)	Ru(2)−C(3)	1.871(4)
Ru(1)−S	2.3795(10)	Ru(2)−C(4)	1.859(4)	Ru(1)−N(1)	2.095(3)	N(1)−N(2)	1.375(4)
Ru(1)−C(1)	1.906(4)	C(1)−O(1)	1.136(6)	Ru(1)−C(2)	1.865(4)	C(2)−O(2)	1.144(5)
Ru(2)−P(2)	2.4261(10)	C(3)−O(3)	1.146(5)	Ru(2)−S	2.4276(10)	C(4)−O(4)	1.139(5)

Bond Angles for **10**

Ru(2)−Ru(1)−P(1)	103.54(3)	Ru(1)−Ru(2)−C(4)	92.43(12)	Ru(1)−Ru(2)−P(2)	157.30(3)	C(3)−Ru(2)−C(4)	87.34
Ru(1)−S−Ru(2)	69.69(3)	N(2)−Ru(2)−C(4)	162.97(4)	C(1)−Ru(1)−C(2)	88.32(18)	Ru(1)−C(1)−O(1)	171.2(4)
Ru(2)−Ru(1)−C(1)	154.94(12)	Ru(1)−C(2)−O(2)	176.0(4)	Ru(2)−Ru(1)−C(2)	102.05(12)	Ru(2)−C(3)−O(3)	179.2(4)
C(2)−Ru(1)−N(1)	172.98(15)	Ru(2)−C(4)−O(4)	175.5(4)	Ru(1)−Ru(2)−C(3)	102.52(12)		

Bond Lengths for **11**

Ru(1)−Ru(2)	2.738(1)	Ru(2)−N(2)	2.120(3)	Ru(1)−P(3)	2.416(1)	Ru(2)−N(4)	2.169(3)
Ru(1)−P(4)	2.309(1)	Ru(2)−C(2)	1.828(4)	Ru(1)−N(1)	2.136(3)	C(1)−O(1)	1.150(5)
Ru(1)−N(3)	2.112(3)	C(2)−O(2)	1.168(5)	Ru(1)−C(1)	1.846(4)	N(1)−N(2)	1.368(4)
Ru(2)−P(1)	2.386(1)	N(3)−N(4)	1.371(4)	Ru(2)−P(2)	2.316(1)		

Bond Angles for **11**

Ru(2)−Ru(1)−P(3)	175.6(1)	P(1)−Ru(2)−P(2)	72.0(1)	P(3)−Ru(1)−P(4)	72.3(1)	P(2)−Ru(2)−N(2)	177.5(1)
P(4)−Ru(1)−N(3)	176.1(1)	C(2)−Ru(2)−N(4)	164.5(2)	C(1)−Ru(1)−N(1)	157.5(1)	C(2)−Ru(2)−N(2)	88.7(1)
C(1)−Ru(1)−N(3)	95.6(1)	Ru(1)−C(1)−O(1)	176.7(3)	Ru(1)−Ru(2)−P(1)	172.3(1)	Ru(2)−C(2)−O(2)	178.4(3)

Bond Lengths for **12**

Ru(1)−Ru(2)	2.701(1)	Ru(2)−C(25)	2.009(6)	Ru(1)−C(25)	2.016(9)	Ru(2)−N(6)	2.093(5)
Ru(1)−C(24)	2.009(6)	Ru(2)−N(3)	2.192(4)	Ru(1)−N(2)	2.194(7)	Ru(2)−N(4)	2.192(6)
Ru(1)−N(1)	2.196(5)	C(26)−O(3)	1.136(9)	N(5)−N(6)	1.365(8)	C(27)−O(4)	1.133(10)
Ru(1)−N(5)	2.097(5)	C(25)−O(2)	1.178(9)	Ru(2)−C(24)	2.033(8)	C(24)−O(1)	1.184(8)
Ru(2)−C(27)	1.866(8)	Ru(1)−C(26)	1.868(7)				

Bond Angles for **12**

Ru(1)−C(24)−Ru(2)	83.9(3)	N(1)−Ru(1)−N(2)	74.2(2)	C(24)−Ru(2)−C(25)	92.9(3)	N(3)−Ru(2)−N(4)	74.0(2)
C(24)−Ru(1)−C(25)	93.4(3)	N(5)−Ru(1)−C(26)	174.5(3)	C(24)−Ru(2)−N(4)	170.4(2)	N(6)−Ru(2)−C(27)	174.6(3)
C(24)−Ru(1)−N(1)	169.4(3)	Ru(1)−C(26)−O(3)	177.4(8)	C(25)−Ru(2)−N(3)	167.9(3)	Ru(2)−C(27)−O(4)	177.6(8)
C(25)−Ru(1)−N(2)	168.9(2)	Ru(1)−C(25)−Ru(2)	84.3(3)				

Bond Lengths for **14A**

Ru(1)−Ru(2)	2.6953(5)	Ru(2)−C(6)	2.016(4)	Ru(1)−C(6)	2.008(5)	Ru(2)−N(4)	2.132(4)
Ru(1)−C(5)	2.024(4)	Ru(2)−N(5)	2.209(4)	Ru(1)−N(2)	2.197(4)	Ru(2)−N(6)	2.196(4)
Ru(1)−N(1)	2.185(4)	C(1)−O(1)	1.136(6)	N(3)−N(4)	1.383(5)	C(2)−O(2)	1.149(6)
Ru(1)−N(3)	2.124(4)	C(5)−O(5)	1.177(5)	Ru(2)−C(5)	2.017(4)	C(6)−O(6)	1.182(5)
Ru(2)−C(2)	1.862(5)	Ru(1)−C(1)	1.880(5)				

Bond Angles for **14A**

Ru(1)−C(5)−Ru(2)	83.7(2)	N(1)−Ru(1)−N(2)	74.23(14)	C(5)−Ru(2)−C(6)	94.6(2)	N(5)−Ru(2)−N(6)	73.71(14)
C(5)−Ru(1)−C(6)	94.6(2)	N(3)−Ru(1)−C(1)	172.5(2)	C(5)−Ru(2)−N(5)	169.3(2)	N(4)−Ru(2)−C(2)	171.5(2)
C(5)−Ru(1)−N(2)	170.6(2)	Ru(1)−C(1)−O(1)	176.8(4)	C(6)−Ru(2)−N(6)	168.6(2)	Ru(2)−C(2)−O(2)	176.0(4)
C(6)−Ru(1)−N(1)	167.6(2)	Ru(1)−C(6)−Ru(2)	84.1(2)				

Bond Lengths for **15**

Ru(1)−Ru(2)	2.685(1)	Ru(2)−N(3)	2.198(4)	Ru(1)−N(6)	2.103(4)	Ru(2)−N(4)	2.185(4)
Ru(1)−N(2)	2.191(4)	Ru(2)−N(5)	2.141(5)	Ru(1)−C(3)	2.026(6)	Ru(2)−C(2)	1.851(7)
Ru(1)−C(1)	1.873(6)	Ru(2)−C(3)	1.997(6)	C(1)−O(1)	1.134(8)	Ru(2)−C(4)	2.025(6)
Ru(1)−C(4)	2.013(6)	C(2)−O(2)	1.144(9)	C(4)−O(4)	1.175(8)	N(5)−N(6)	1.393(6)
C(3)−O(3)	1.188(8)	Ru(1)−N(1)	2.200(4)				

Table 1 (Continued)

Bond Angles for **15**

Ru(1)−C(3)−Ru(2)	83.7(2)	N(1)−Ru(1)−N(2)	75.6(2)	C(3)−Ru(2)−C(4)	95.2(2)	N(3)−Ru(2)−N(4)	75.0(2)
C(3)−Ru(1)−C(4)	94.7(2)	N(6)−Ru(1)−C(1)	172.7(2)	C(3)−Ru(2)−N(4)	169.4(2)	N(5)−Ru(2)−C(2)	173.6(2)
C(3)−Ru(1)−N(2)	168.8(2)	Ru(1)−C(1)−O(1)	176.8(6)	C(4)−Ru(2)−N(3)	168.1(2)	Ru(2)−C(2)−O(2)	178.5(6)
C(4)−Ru(1)−N(1)	171.1(2)	Ru(1)−C(4)−Ru(2)	83.4(2)				

Bond Lengths for **16**

Ru(1)−I(1)	2.731(2)	Ru(2)−N(2)	2.113(11)	I(2)−I(3)	2.926(2)	Ru(2)−N(4)	2.147(13)
Ru(2)−I(1)	2.733(1)	Ru(2)−C(9)	1.868(16)	I(3)−I(4)	2.902(2)	Ru(2)−C(10)	1.903(20)
Ru(1)−P(1)	2.386(4)	C(7)−O(1)	1.131(19)	Ru(1)−N(1)	2.123(13)	C(8)−O(2)	1.153(25)
Ru(1)−N(3)	2.105(10)	C(9)−O(3)	1.140(21)	Ru(1)−C(7)	1.877(15)	C(10)−O(4)	1.124(24)
Ru(1)−C(8)	1.869(20)	N(1)−N(2)	1.360(16)	Ru(2)−P(2)	2.398(4)	N(3)−N(4)	1.347(16)

Bond Angles for **16**

Ru(1)−I(1)−Ru(2)	87.1(1)	C(7)−Ru(1)−C(8)	90.8(7)	I(1)−Ru(1)−P(1)	177.5(1)	C(9)−Ru(2)−C(10)	89.6(8)
I(1)−Ru(2)−P(2)	178.9(1)	Ru(1)−C(7)−O(1)	175.8(14)	I(2)−I(3)−I(4)	173.9(1)	Ru(1)−C(8)−O(2)	173.9(14)
N(1)−Ru(1)−N(3)	88.2(4)	Ru(2)−C(9)−O(3)	174.1(11)	N(2)−Ru(2)−N(4)	88.7(5)	Ru(2)−C(10)−O(4)	174.0(17)

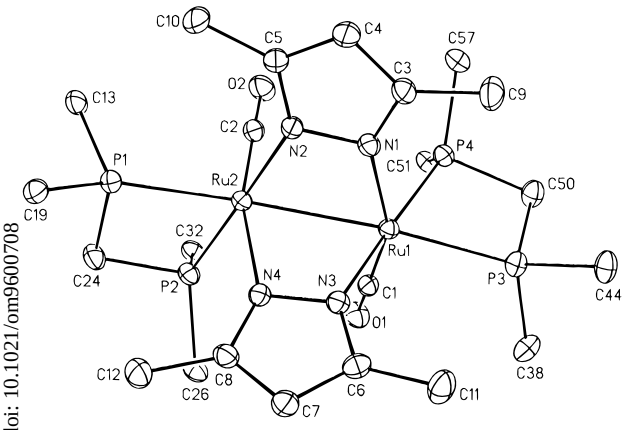

Figure 4. ORTEP plot of **11** with 50% probability ellipsoids. Only the *ipso*-carbon atoms of the phenyl groups of dppm are shown for clarity.

Scheme 4

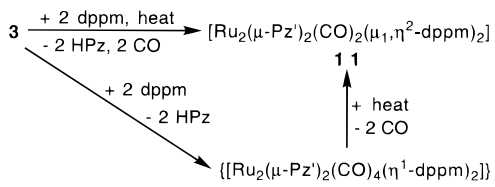

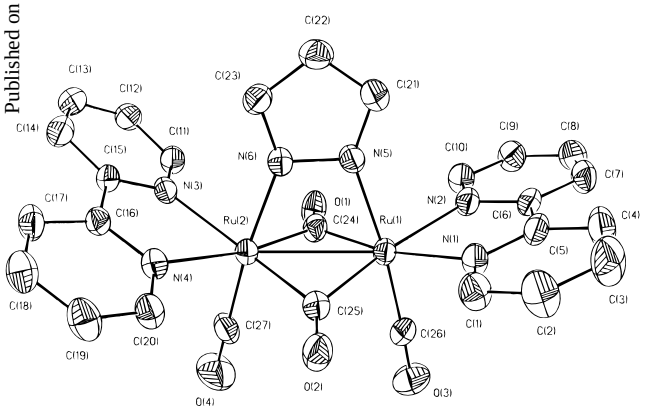

Figure 5. ORTEP plot of [**12**]$^+$ with 30% thermal ellipsoids.

Consistent with the structure of **10** (Figure 3b), phosphine groups can occupy the equatorial sites if necessary.

However, excepting the replacement of the axial HL groups, the less-flexible bidentate ligands such as bpy and phen can cleave one μ-O_2CMe or μ-L bridge, but without losing any carbonyl in **1**−**3**, to afford [Ru_2(μ-L)(μ-CO)$_2$(CO)$_2$(μ_1,η^2-(N−N))$_2$]$^+$ (L = Pz, N−N = bpy ([**12**]$^+$), phen ([**13**]$^+$); L = Pz′, N−N = bpy ([**14**]$^+$), phen ([**15**]$^+$)) (Scheme 5). The crystal structures of **12**, **14**, and **15** were carried out to confirm the formulation, and it was found that in each asymmetric unit of the crystal used were two similar diruthenium molecules, **14A** and **14B**, found for **14**, although only one dimer was observed for **12** and **15**. The structures of [**12**]$^+$, [**14A**]$^+$, and [**15**]$^+$ are shown in Figures 5−7, respectively. Apparently the more severe steric effect required by bpy

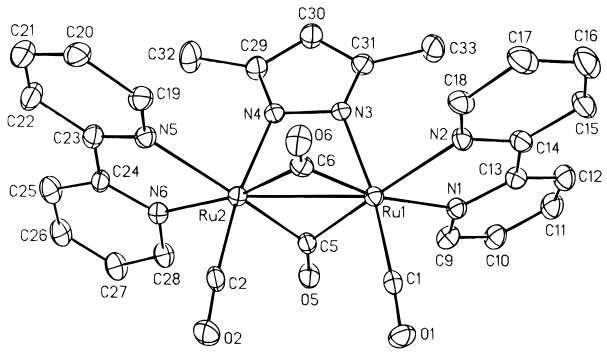

Figure 6. ORTEP plot of [**14A**]$^+$ with 50% probability ellipsoids.

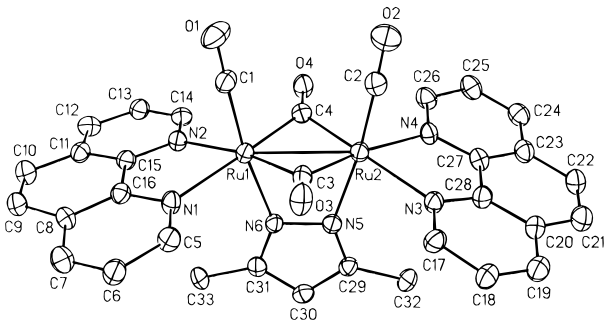

Figure 7. ORTEP plot of [**15**]$^+$ with 50% probability ellipsoids.

Scheme 5

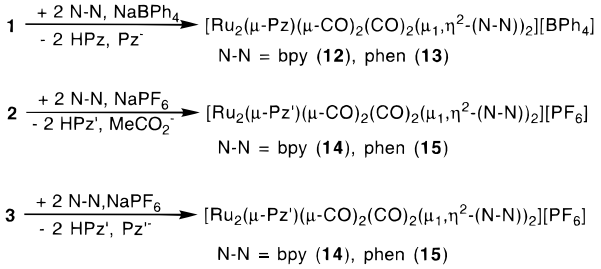

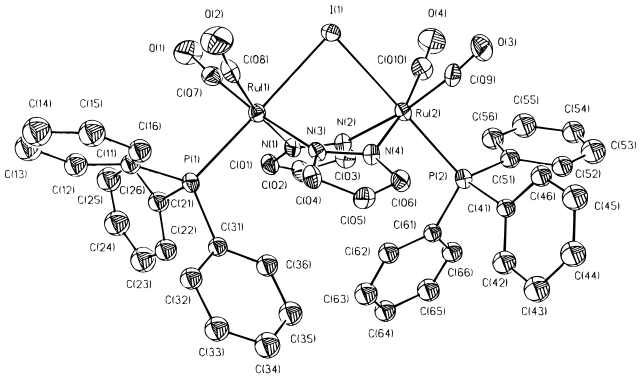

Figure 8. ORTEP plot of [**16**]$^+$ with 50% probability ellipsoids.

and phen, relative to dppm,[5,6] results in a geometry in **12**−**15** totally different from that in **11**.

The μ-O_2CMe linkage was previously reported to be cleavable, and the product $[Ru_2(\mu\text{-}O_2CMe)(\mu\text{-}CO)_2(CO)_2(\mu_1,\eta^2\text{-}(N{-}N))_2]^+$ can be obtained from the reaction of *catena*-$[Ru(O_2CMe)(CO)_2]$ with bpy or phen in EtOH.[7] Here we wish to add that the apparently strong μ-L linkage, previously reported to be a stable bridge in all dirhodium and -iridium complexes,[1] can be *cleaved*. The reaction between the heterobridged dimer **2** and N−N did not give a mixture of $[Ru_2(\mu\text{-}O_2CMe)(\mu\text{-}CO)_2(CO)_2(\mu_1,\eta^2\text{-}(N{-}N))_2]^+$ and $[Ru_2(\mu\text{-L})(\mu\text{-}CO)_2(CO)_2(\mu_1,\eta^2\text{-}(N{-}N))_2]^+$ but only the latter one, consistent with the weaker μ-acetato linkage compared with the μ-Pz′ linkage, and the cleaving process is also selective when bpy or phen is used.

The comparable Ru−Ru distances of 2.701(1) Å in [**12**]$^+$, 2.6953(5) Å in [**14A**]$^+$, 2.6988(5) Å in [**14B**]$^+$, 2.685(1) Å in [**15**]$^+$, 2.701(1) Å in $[Ru_2(\mu\text{-}O_2CMe)(\mu\text{-}CO)_2(CO)_2(\mu_1,\eta^2\text{-bpy})_2]^+$,[7a] and 2.709(1) Å in $[Ru_2(\mu\text{-}O_2CMe)(\mu\text{-}CO)_2(CO)_2(\mu_1,\eta^2\text{-phen})_2]^+$ [7b] can be attributed to the similar flexibility of two bidentate ligands bpy and phen with the averaged torsion angles ∠N−C−C−N, such as ∠N(3)−C(15)−C(16)−N(4) in **12**, less than 6.4°. The identical distance of 2.701(1) Å found in both cations **12**$^+$ and $[Ru_2(\mu\text{-}O_2CMe)(\mu\text{-}CO)_2(CO)_2(\mu_1,\eta^2\text{-bpy})_2]^+$ probably indicates a μ-O_2CMe linkage in a steric bulk similar to a μ-Pz linkage and further supports the facile replacement of two μ-O_2CMe linkages in **1** by μ-Pz groups to give **4** (Scheme 1).

Reactions with Electrophiles. Electrophiles such as I_2 can react with **4**. However, it was strange to find that the reaction should consume up to 2 equiv of I_2 to complete the reaction for every dinuclear compound **4**. Later, the crystal structure of the product compound was revealed to have an I_3^- as a counterion for $[Ru_2(\mu\text{-}Pz)_2(\mu\text{-}I)(CO)_4(PPh_3)_2]^+$ ([**16**]$^+$; cf., Figure 8 and Scheme 6). Though with two μ-Pz linkages, the two Ru atoms are separated by 3.762(2) Å, indicating no metal−metal bonding interactions. Obviously, the electrophilic reagent I_2 can cleave the Ru−Ru bond and raise the oxidation state of each Ru atom, but cannot break the μ-azolato linkage. Such a feature was previously observed in the dirhodium and -iridium systems[1] but not yet reported in the diruthenium system.[2] From the crystal structures of **2**, **5**, **10**−**12**, and **14**−**16**, it is apparent that the μ-azolato linkage is flexible to maintain two metal fragments in close proximity, both within and beyond the requirements of metal−metal interactions in the dimetal system.

Scheme 6

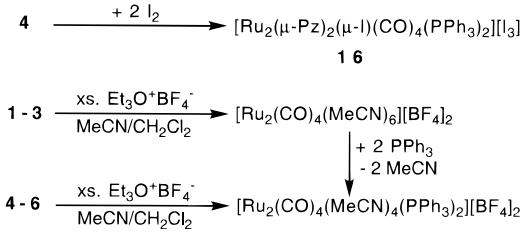

From the aforementioned results, one or two μ-azolato linkages in **1**−**3** appear to be able to survive during a nucleophilic or electrophilic reaction (Schemes 1−5). However, some other reactions are present enabling removal of all the μ-acetato and -azolato linkages in the compounds.

An electrophilic reagent such as $Et_3O^+BF_4^-$ in the presence of MeCN was previously reported by our laboratory to convert a series of $[Ru_2(CO)_4(\mu\text{-}O_2CMe)_2(L')_2]$ (L′ = MeCN or phosphine (PR_3)) into $[Ru_2(CO)_4(MeCN)_6][BF_4]_2$ and $[Ru_2(CO)_4(MeCN)_4(PR_3)_2][BF_4]_2$, probably involving an abstraction reaction by transformation of a μ-acetato bridge into the weakly coordinating ethyl acetate.[4b] We found that a similar reaction also occurs for **1**−**3** and **4**−**6** into $[Ru_2(CO)_4(MeCN)_6][BF_4]_2$ and $[Ru_2(CO)_4(MeCN)_4(PPh_3)_2][BF_4]_2$, respectively. The former product, $[Ru_2(CO)_4(MeCN)_6][BF_4]_2$, can be converted by adding PPh_3 into the latter one, $[Ru_2(CO)_4(MeCN)_4(PPh_3)_2][BF_4]_2$ (Scheme 6).[4a]

Conclusion

Our investigation into the diruthenium carbonyl complexes containing the μ-azolato linkage resulted in the specific synthesis of **1**−**3** in satisfactory yield. Both nucleophilic and electrophilic reactions of **1**−**3** produce selectively one type of product containing either hetero- or homobridges (Schemes 1−6) as confirmed in eight X-ray crystal structures (Figures 1−8). The μ-azolato linkage has been demonstrated to promote formation of novel compounds such as **11** and to maintain two ruthenium fragments in close proximity, both within and beyond the requirements of metal−metal interactions. More importantly, if necessary, the μ-azolato linkages can be cleaved partially by using the less-flexible bidentate nucleophiles such as bpy or phen or removed totally by using electrophiles such as trialkyloxonium reagents. The latter reaction can produce potentially versatile compounds such as $[Ru_2(CO)_4(MeCN)_6][BF_4]_2$ and $[Ru_2(CO)_4(MeCN)_4(PPh_3)_2][BF_4]_2$.[4]

Experimental Section

General Comments. All solvents were dried and purified by standard methods [ethers, paraffins, and arenes from potassium with benzophenone as indicator; halocarbons and acetonitrile from CaH_2; alcohols from the corresponding alkoxide] and were freshly distilled under nitrogen immediately before use. All reactions and manipulations were carried out in standard Schlenk ware, connected to a switchable double

(6) (a) Puddephatt, R. J. *Chem. Soc. Rev.* **1983**, *12*, 99. (b) Balch, A. L. *Homogeneous Catalysis with Metal Phosphine Complexes*; Pignolet, L. H., Ed.; Plenum: New York, 1983; pp 167−213. (c) Chaudret, B.; Delavaux, B.; Poilblanc, R. *Coord. Chem. Rev.* **1988**, *86*, 191.

(7) (a) Steyn, M. M. d. V.; Singleton, E. *Acta Crystallogr.* **1988**, *C44*, 1722. (b) Frediani, P.; Bianchi, M.; Salvini, A.; Guarducci, R.; Carluccio, L. C.; Piacenti, F.; Ianelli, S.; Nardelli, M. *J. Organomet. Chem.* **1993**, *463*, 187.

manifold providing vacuum and nitrogen. Reagents and phosphines were used as supplied by either Aldrich or Strem. ^{1}H and ^{31}P NMR spectra were measured on a Bruker AM-200 (^{1}H, 200 MHz), Bruker AMC-400, or Varian Unity Plus-400 (^{1}H, 400 MHz; ^{31}P, 162 MHz) NMR spectrometer. ^{1}H chemical shifts (δ in ppm, J in Hz) are defined as positive downfield relative to internal $MeSi_4$ (TMS) or the deuterated solvent, while ^{31}P chemical shifts are defined as positive downfield relative to external 85% H_3PO_4. The IR spectra were recorded on a Hitachi Model 270−30 or Bio-Rad FTS 175 instrument. The following abbreviations were used: s, strong; m, medium; w, weak; s, singlet; d, doublet; t, triplet; dd, doublet of doublet; br, broad unresolved signal. Microanalyses were carried out by the staff of the Microanalytical Service of the Department of Chemistry, National Cheng Kung University.

Synthesis of $[Ru_2(CO)_4(\mu\text{-}Pz)_2(HPz)_2]$ (1). In a 100-mL Schlenk flask was added *catena*-$[Ru(O_2CMe)(CO)_2]$ (1.0 g, 2.33 mmol), HPz (0.83 g, 12.2 mmol), 5 mL of Et_3N, and 30 mL of EtOH at room temperature. The mixture was then heated under reflux for 2 h and cooled to room temperature. The solvent and Et_3N were removed under vacuum and the resulting solid residue was redissolved in 5 mL of MeOH. Upon addition of 50 mL of H_2O, a milky yellow precipitate formed immediately, which was collected on a medium frit. Recrystallization from CH_2Cl_2/MeOH afforded the pure product in 91% yield. Alternatively, as described below for **3**, **1** can also be prepared from $[Ru_2(CO)_4(MeCN)_6][BF_4]_2$ and HPz/Et_3N. Anal. Calcd for $C_{16}H_{14}N_8O_4Ru_2$: C, 32.88; H, 2.41; N, 19.17. Found: C, 32.54; H, 2.39; N, 18.85. ^{1}H NMR (25 °C, 400 MHz, acetone-d_6): NH at 12.87 (br, 2 H); H^3 or H^5 on HPz at 8.10 (m, 2 H), 7.83 (m, 2 H); H^3 and H^5 on μ-Pz at 7.09 (m, 4 H); H^4 on HPz at 6.64 (m, 2 H,); H^4 on μ-Pz at 6.02 (m, 2 H). IR: ν_{CO}, 2024 s, 1976 m, 1942 s cm^{-1} in CH_2Cl_2; ν_{NH}, 3436 w; ν_{CO}, 2016 s, 1964 m, 1934 s cm^{-1} in KBr.

Synthesis of $[Ru_2(CO)_4(\mu\text{-}Pz')(\mu\text{-}O_2CMe)(HPz')_2]$ (2). The yellow compound **2** was prepared from *catena*-$[Ru(O_2CMe)(CO)_2]$ using HPz′ in a procedure similar to that used for **1**. The yield is 87%. Anal. Calcd for $C_{21}H_{16}N_6O_6Ru_2$: C, 38.18; H, 3.97; N, 12.72. Found: C, 38.51; H, 3.99; N, 12.39. ^{1}H NMR (25 °C, 200 MHz, $CDCl_3$): NH at 10.92 (br, 2 H); H^4 on HPz′ at 6.02 (s, 1 H), 6.01 (s, 1 H); H^4 on μ-Pz′ at 5.57 (s, 1 H); Me^3 or Me^5 on HPz′ at 2.48 (br, 6 H), 2.29 (br, 6 H); Me^3 or Me^5 on μ-Pz′ at 1.38 (br, 6 H); μ-O_2C**Me** at 2.15 (s, 3 H). IR: ν_{CO}, 2024 s, 1974 m, 1940 s cm^{-1} in CH_2Cl_2; ν_{NH}, 3328 w, ν_{CO}, 2024 s, 1970 m, 1942 s cm^{-1} in KBr.

Synthesis of $[Ru_2(CO)_4(\mu\text{-}Pz')_2(HPz')_2]$ (3). To the solution of $[Ru_2(CO)_4(MeCN)_6][BF_4]_2$, prepared *in situ* by the reaction of $[Ru_2(CO)_4(\mu\text{-}O_2CMe)_2(MeCN)_2]$ (0.28 mmol) with excess $Et_3O^+BF_4^-$,[4] in a 100-mL Schlenk flask was added HPz′ (0.14 g, 1.4 mmol), 1 mL of Et_3N, and 20 mL of MeOH at room temperature. The mixture was then heated under reflux for 2 h and cooled to room temperature. The volume of the solution was reduced to *ca.* 5 mL under vacuum. Upon addition of 40 mL of H_2O, a milky yellow precipitate formed immediately, which was collected on a medium frit. Recrystallization from CH_2Cl_2/MeOH afforded the pure product in 83% yield. Anal. Calcd for $C_{24}H_{30}N_8O_4Ru_2$: C, 41.38; H, 4.34; N, 16.08. Found: C, 41.35; H, 4.28; N, 15.83. ^{1}H NMR (25 °C, 200 MHz, $CDCl_3$): NH at 9.80 (br, 2 H); H^4 on HPz′ at 6.05 (s, 1 H), 5.81 (s, 1 H); H^4 on μ-Pz′ at 5.31 (s, 1 H); Me^3 or Me^5 on HPz′ at 2.55 (br, 6 H), 2.24 (br, 6 H); Me^3 or Me^5 on μ-Pz′ at 1.55 (br, 12 H). IR: ν_{CO}, 2016 s, 1968 m, 1934 s cm^{-1} in CH_2Cl_2; ν_{NH}, 3424 w, ν_{CO}, 2012 s, 1960 m, 1928 s cm^{-1} in KBr.

Reaction between 1 and PPh_3. In a 100-mL Schlenk flask was added **1** (0.100 g, 0.17 mmol), PPh_3 (0.18 g, 0.69 mmol), and 25 mL of MeCN at room temperature. The solution gradually formed pale yellow precipitate. After 0.5 h, the yellow solid was collected on a medium frit, washed three times with 5 mL of MeCN, and dried in vacuo to give 0.096 g (80%). This solid was identified as $[Ru_2(CO)_4(\mu\text{-}Pz)_2(PPh_3)_2]$ by comparison of both the NMR and IR spectral evidences with those reported.[2c]

Reaction between 2 and PPh_3. The yellow compound **5** was prepared from **2** in a procedure similar to that used for **4**. The yield is 97%. Anal. Calcd for $C_{47}H_{40}N_2O_6P_2Ru_2$: C, 56.85; H, 4.06; N, 2.82. Found: C, 56.78; H, 4.04; N, 2.72. ^{1}H NMR (25 °C, 200 MHz, $CDCl_3$): PPh_3 at 7.60 (br, 12 H), 7.40 (m, 18 H); H^4 on μ-Pz′ at 5.67 (s, 1 H); Me^3 or Me^5 on μ-Pz′ at 1.57 (br, 6 H); μ-O_2C**Me** at 1.75 (s, 3 H). ^{31}P{^{1}H} NMR (25 °C, 162 MHz, $CDCl_3$): 12.50 (s, 2 P). IR (CH_2Cl_2): ν_{CO}, 2028 s, 1982 m, 1954 s cm^{-1}.

Reaction between 3 and PPh_3. The yellow compound **6** was prepared from **3** in a procedure similar to that used for **4**. The yield is 94%. Anal. Calcd for $C_{50}H_{44}N_4O_4P_2Ru_2$: C, 58.36; H, 4.31; N, 5.44. Found: C, 58.29; H, 4.28; N, 5.57. ^{1}H NMR (25 , 200 MHz, $CDCl_3$): PPh_3 at 7.54−7.23 (m, 30 H); H^4 on μ-Pz′ at 5.63 (s, 1 H), 5.58 (s, 1 H); Me^3 or Me^5 on μ-Pz′ at 2.27 (s, 3 H), 1.80 (s, 3 H), 1.51 (s, 3 H), 1.46 (s, 3 H). ^{31}P{^{1}H} NMR (25 °C, 162 MHz, $CDCl_3$): 12.69 (s, 2 P). IR (CH_2Cl_2): ν_{CO}, 2016 s, 1990 m, 1944 s, 1924 m cm^{-1}.

Reaction between 1 and dppm. The yellow compound **7** was prepared from **1** using dppm in a procedure similar to that used for **4**. The yield is 93%. Anal. Calcd for $C_{60}H_{50}N_4O_4P_4Ru_2$: C, 59.22; H, 4.14; N, 4.60. Found: C, 59.28; H, 4.08; N, 4.59. ^{1}H NMR (25 °C, 200 MHz, $CDCl_3$): PPh_3 at 7.65−7.10 (m, 40 H); H^3 and H^5 on μ-Pz at 6.46 (d, 4 H, J = 2.2); H^4 on μ-Pz at 5.63 (t, 2 H); CH_2 of dppm at 3.47 (m, 4 H). ^{31}P{^{1}H} NMR (25 °C, 162 MHz, $CDCl_3$): 12.12 (m, 2 P), −26.18 (m, 2 P). IR (CH_2Cl_2): ν_{CO}, 2024 s, 1982 m, 1954 s cm^{-1}.

Reaction between 5 and NaPz, NaSPh, and NaS^{t}Bu. A typical reaction is shown as follows. In a 100-mL Schlenk flask was added **5** (108 mg, 0.109 mmol), NaPz (0.30 g, 3.33 mmol), and 20 mL of THF at room temperature. The mixture was then heated under reflux for 4 h and cooled to room temperature. The solvent was removed under vacuum. Recrystallization from CH_2Cl_2/hexane afforded the pure product (**8**) in 85% yield. Anal. Calcd for $C_{48}H_{40}N_4O_4P_2Ru_2$: C, 57.59; H, 4.02; N, 5.59. Found: C, 57.65; H, 3.91; N, 5.54. ^{1}H NMR (25 °C, 200 MHz, $CDCl_3$): PPh_3 at 7.57 (br, 12 H), 7.39 (br, 18 H); H^3 and H^5 on μ-Pz at 6.89 (d, 2 H, J = 2.0); H^4 on μ-Pz at 5.78 (t, 1 H); H^4 on μ-Pz′ at 5.61 (s, 1 H); Me^3 and Me^5 on μ-Pz′ at 1.56 (s, 6 H). ^{31}P{^{1}H} NMR (25 °C, 162 MHz, $CDCl_3$): 12.12 (s, 2 P). IR (CH_2Cl_2): ν_{CO}, 2028 s, 1986 m, 1958 s cm^{-1}. Compound **9** was prepared from **5** using NaSPh in a procedure similar to that used for **8**. The yield is 87%. Anal. Calcd for $C_{51}H_{42}N_2O_4P_2Ru_2S$: C, 58.72; H, 4.05; N, 2.69. Found: C, 58.76; H, 3.94; N, 2.78. ^{1}H NMR (25 °C, 200 MHz, $CDCl_3$): PPh_3 at 7.38 (br, 12 H), 7.27 (m, 18 H); SPh at 6.81 (m, 5 H); H^4 on μ-Pz′ at 5.42 (s, 1 H); Me^3 and Me^5 on μ-Pz′ at 1.26 (s, 6 H). ^{31}P{^{1}H} NMR (25 °C, 162 MHz, $CDCl_3$): 24.66 (s, 2 P). IR (CH_2Cl_2) ν_{CO}, 2016 s, 1982 m, 1946 s cm^{-1}. Compound **10** was prepared from **5** using NaS^{t}Bu in a procedure similar to that used for **8**. The yield is 90%. Anal. Calcd for $C_{49}H_{44}N_2O_4P_2Ru_2S$: C, 57.53; H, 4.53; N, 2.74. Found: C, 57.33; H, 4.34; N, 2.69. ^{1}H NMR (25 °C, 200 MHz, $CDCl_3$): PPh_3 at 7.55−7.26 (m, 30 H); H^4 on μ-Pz′ at 5.23 (s, 1 H); Me^3 and Me^5 on μ-Pz′ at 1.54 (br, 6 H); S^{t}Bu at 1.12 (s, 9 H). ^{31}P{^{1}H} NMR (25 °C, 162 MHz, $CDCl_3$): 22.46 (d, 1 P, J = 8.7), 41.9 (d, 1 P). IR (CH_2Cl_2): ν_{CO}, 2004 s, 1980 vs, 1934 s cm^{-1}.

Reaction between 3 and dppm. In a 100-mL Schlenk flask was added **3** (133 mg, 0.191 mmol), dppm (168 mg, 0.438 mmol), and 30 mL of THF at room temperature. The mixture was first stirred at this temperature for 10 min and then heated under reflux for 28 h, giving a clear orange-red solution. The solvent was removed under vacuum and the resulting solid redissolved in 40 mL of CH_2Cl_2. After filtration through a medium frit, the volume of the filtrate was reduced to ca. 15 mL. A 45 mL volume of hexane was carefully added on the top of the solution and the two-layer mixture was cooled to −40 °C for 1 week, giving orange-red crystals. The crystals were collected on a medium frit and dried in vacuo to give 157 mg of $[Ru_2(\mu\text{-}Pz')_2(CO)_2(\mu_1,\eta^2\text{-dppm})_2]$ (**11**), containing a solvate

Table 2. Crystal Data

	compd			
	2	**5**	**10**	**11**
formula	$C_{21}H_{26}N_6O_6Ru_2$	$C_{47}H_{40}N_2O_6P_2Ru_2$	$C_{49}H_{46}N_2O_4P_4Ru_2S$	$C_{63}H_{60}Cl_2N_4O_2P_4Ru_2$
fw	660.61	992.92	1023.05	1302.1
color, habit	yellow, prism	orange, prism	orange, prism	orange, equant
diffractometer used	Rigaku AFC6S	Nonius CAD4	Nonium CAD4	Siemens SMART-CCD
space group	monoclinic,$P\,2_1/c$	monoclinic,$P2_1/c$	monoclinic, $P2_1/n$	monoclinic, $P2_1/n$
a, Å	14.069(5)	10.4555(16)	13.0086(18)	13.970(3)
b, Å	13.288(3)	16.113(3)	17.363(3)	25.737(5)
c, Å	14.545(3)	26.063(4)	20.945(3)	16.826(3)
β, deg	98.25(2)	91.420(13)	104.251(12)	92.65(3)
V, Å^3	2691(1)	4389.6(13)	4585.3(12)	6043(2)
Z	4	4	4	4
D_{calcd}, g cm^{-3}	1.630	1.502	1.482	1.431
λ(Mo Kα), Å	0.710 69	0.710 69	0.710 69	0.710 73
F(000)	1320	1998	2070	2656
unit cell detn: no. 2θ range, deg	20, 8−12	25, 17−23	25, 17−26	whole data
scan type	ω−2θ	θ−2θ	θ−2θ	hemisphere
2θ range, deg	6−50	2−50	2−50	1−52
h,k,l range	16,15,±17	±12,19,30	±15,20,24	±17,31,20
μ(Mo Kα), cm^{-1}	11.67	7.89	7.57	7.40
cryst size, mm	0.41 × 0.41 × 0.66	0.20 × 0.20 × 0.30	0.30 × 0.35 × 0.35	0.4 × 0.4 × 0.4
temp, K	296	298	298	297
no. of measd reflns	5228	4227	8063	27 384
no. of unique reflns	5014	4227	8063	10 543
no. of obsd reflns (N_o)	3407 (>3σ)	2345 (>2σ)	5956 (>2σ)	7883 (>3σ)
R,[a] R_w[a]	0.047, 0.048	0.044, 0.041	0.031, 0.031	0.038, 0.038
GOF[a]	4.00	1.08	1.28	1.70
refinement program	TEXSAN	NRCVAX	NRCVAX	SHELXTL-PLUS
no. of ref params (N_p)	316	532	542	695
weighting scheme	$[\sigma^2(F_o)]^{-1}$	$[\sigma^2(F_o) + 0.0002F_o^2]^{-1}$	$[\sigma^2(F_o) + 0.0001F_o^2]^{-1}$	$[\sigma^2(F_o) + 0.0001F_o^2]^{-1}$
g (2nd ext coeff) × 10e^4	0	0	0.95(4)	0.000052(8)
$(\Delta\rho)_{max}$, e Å^{-3}	0.79	0.40	0.44	0.42
$(\Delta\rho)_{min}$, eÅ^{-3}	−1.28	−0.41	−0.36	−0.44

	compd			
	12	**14**	**15**	**16**
formula	$C_{52}H_{41}BCl_2N_6O_4Ru_2$	$C_{59}H_{48}Cl_2F_{12}N_{12}O_8P_2Ru_4$	$C_{34}H_{25}Cl_2F_6N_2O_4PRu_2$	$C_{47.5}H_{36}Cl_3I_4N_4O_4P_2Ru_2$
fw	1097.8	1818.21	999.6	1604.8
color, habit	orange, rhombohedron	orange, equant	yellow-brown, lamellar	orange-brown, irregular
diffractometer used	Siemens SMART-CCD	Siemens SMART-CCD	Siemens SMART-CCD	Siemens P4
space group	triclinic, $P\bar{1}$	triclinic, $P\bar{1}$	orthorhombic, $Pbca$	triclinic, $P\bar{1}$
a, Å	10.712(4)	14.4764(2)	17.614(2)	11.744(1)
b, Å	13.939(4)	15.0429(2)	13.624(2)	13.357(1)
c, Å	17.871(7)	17.0034(1)	31.294(2)	20.173(2)
α, deg	67.156(14)	97.829(1)	90	93.19(1)
β, deg	84.40(2)	106.942(1)	90	95.09(1)
γ, deg	85.273(16)	103.125(1)	90	112.90(1)
V, Å^3	2444.5(17)	3367.16(7)	7509.6(15)	2889.3(4)
Z	2	2	8	2
D_{calcd}, g cm^{-3}	1.491	1.793	1.768	1.845
λ(Mo Kα), Å	0.710 73	0.710 73	0.710 73	0.710 73
F(000)	1108	1796	3952	1524
unit cell detn: no. 2θ range, deg	whole data	whole data	whole data	25, 24 < 2θ < 25
scan type	hemisphere	hemisphere	hemisphere	θ−ω
2θ range, deg	3−47	3−51	3−53	4−45
h,k,l range	±11,±15,19	±17,±17,20	20,16,36	12,±14,±21
μ(Mo Kα), cm^{-1}	7.78	11.02	10.66	28.96
cryst size, mm	0.3 × 0.3 × 0.4	0.48 × 0.45 × 0.38	0.61 × 0.46 × 0.08	0.15 × 0.3 × 0.4
temp, K	298	296	296	298
no. of measd reflns	9549	19 376	32 873	7994
no. of unique reflns	6877	11 036	6756	7546
no. of obsd reflns (N_o)	5837 (>4σ)	11033 (>2σ)	4934 (>3σ)	4260 (>6σ)
R,[a] R_w[a]	0.055, 0.068	0.040, 0.051	0.047, 0.051	0.048, 0.057
GOF[a]	1.89	1.09	1.34	1.61
refinement program	SHELXTL-PLUS	SHELXTL-PLUS	SHELXTL-PLUS	SHELXTL-PLUS
no. of ref params (N_p)	556	893	497	429
weighting scheme	$[\sigma^2(F_o) + 0.0004F_o^2]^{-1}$	$[\sigma^2(F_o) + 0.0014F_o^2]^{-1}$	$[\sigma^2(F_o) + 0.00014F_o^2]^{-1}$	$[\sigma^2(F_o) + 0.0002F_o^2]^{-1}$
g (2nd ext coeff) × 10e^4	0	0.0024(2)	0.00027(3)	0.00011(2)
$(\Delta\rho)_{max}$, eÅ^{-3}	0.72	0.94	0.95	0.95
$(\Delta\rho)_{min}$, eÅ^{-3}	−0.77	−0.60	−0.51	−0.93

[a] $R = [\sum||F_o| - |F_c||/\sum|F_o|]$. $R_w = [\sum w(|F_o| - |F_c|)^2/\sum w|F_o|^2]^{1/2}$. GOF $= [\sum w(|F_o| - |F_c|)^2/(N_o - N_p)]^{1/2}$.

molecule of CH_2Cl_2, which was later confirmed by the elementary analysis results and the ^{1}H NMR spectral evidence. Yield: 63%. Anal. Calcd for $C_{63}H_{58}Cl_2N_4O_2P_4Ru_2$: C, 58.11; H, 4.64; N, 4.30. Found: C, 58.14; H, 4.67; N, 4.40. ^{1}H NMR (25 °C, 200 MHz, $CDCl_3$): dppm at 7.71−6.99 (m, 40 H), 4.95 (m, 4 H); H^4 on μ-Pz′ at 5.44 (br, 2 H); Me^3 and Me^5 on μ-Pz′

at 2.10 (s, 6 H), 1.15 (s, 6 H). $^{31}P\{^1H\}$ NMR (25 °C, 162 MHz, $CDCl_3$): 11.41 (m, 2 P), −30.26 (m, 2 P). IR (CH_2Cl_2): ν_{CO}, 1914 s, 1892 s cm^{-1}.

Reaction between 1−3 and N−N (N−N = bpy, phen). A typical reaction is shown as follows. In a 100-mL Schlenk flask was added **1** (205 mg, 0.350 mmol), bpy (116 mg, 0.742 mmol), and 25 mL of MeOH at room temperature. The mixture was then heated under reflux for 5 h and then cooled to room temperature. A 252 mg amount of $NaBPh_4$ (0.732 mmol) dissolving in 10 mL of MeCN was added to the mixture, forming a precipitate within 30 min. The solvents were removed under vacuum. Recrystallization from CH_2Cl_2/MeOH gave crude product, which was then washed three times each with 5 mL of MeOH and 5 mL of Et_2O to remove completely the unreacted bpy and dried in vacuo to give 207 mg of pure $[Ru_2(\mu\text{-Pz})(\mu\text{-CO})_2(CO)_2(\mu_1,\eta^2\text{-bpy})_2][BPh_4]$ (**12**) (58%). Anal. Calcd for $C_{51}H_{39}BN_6O_4Ru_2$: C, 60.47; H, 3.88; N, 8.29. Found: C, 60.27; H, 3.78; N, 8.14. ^1H NMR (25 °C, 200 MHz, acetone-d_6): bpy at 10.16 (m, 4 H), 8.92 (m, 4 H), 8.50 (m, 4 H), 8.14 (m, 4 H); BPh_4 at 7.35 (m, 8 H), 6.87 (m, 8 H), 6.75 (m, 4 H); H^3 and H^5 on μ-Pz at 5.80 (d, 2 H, J = 2.2); H^4 on μ-Pz at 5.29 (t, 1 H). IR (CH_2Cl_2): ν_{CO}, 2028 s, 1994 w, 1801 w, 1746 s cm^{-1}. A similar reaction between **1** and phen gave $[Ru_2(\mu\text{-Pz})(\mu\text{-CO})_2(CO)_2(\mu_1,\eta^2\text{-phen})_2][BPh_4]$ (**13**) (68%). Anal. Calcd for $C_{55}H_{39}BN_6O_4Ru_2$: C, 62.26; H, 3.71; N, 7.92. Found: C, 62.03; H, 3.46; N, 8.02. ^1H NMR (25 °C, 200 MHz, acetone-d_6): phen at 10.50 (dd, 4 H, J = 1.4, 5.2), 9.11 (dd, 4 H, J = 1.4, 8.2), 8.49 (dd, 4 H, J = 5.2, 8.2), 8.46 (s, 4 H); BPh_4 at 7.34 (m, 8 H), 6.92 (m, 8 H), 6.75 (m, 4 H); H^3 and H^5 on μ-Pz at 5.34 (d, 2 H, J = 2.0); H^4 on μ-Pz at 5.06 (t, 1 H). IR (CH_2Cl_2): ν_{CO}, 2028 s, 1994 w, 1801 w, 1746 s cm^{-1}. Following a procedure similar to that for **12**, the reaction of **2** and **3** with bpy in the presence of $NaPF_6$ gave only one identical product $[Ru_2(\mu\text{-Pz}')(\mu\text{-CO})_2(CO)_2(\mu_1,\eta^2\text{-bpy})_2][PF_6]$ (**14**) in 73 and 85% yield, respectively. Anal. Calcd for $C_{29}H_{23}F_6N_6O_4PRu_2$: C, 40.19; H, 2.67; N, 9.69. Found: C, 39.88; H, 2.81; N, 9.80. ^1H NMR (25 °C, 200 MHz, $CDCl_3$): bpy at 10.24 (m, 4 H), 8.67 (m, 4 H), 8.38 (m, 4 H), 7.95 (m, 4 H); H^4 on μ-Pz′ at 4.84 (s, 1 H); Me^3 and Me^5 on μ-Pz′ at 3.50 (br, 6 H). IR (CH_2Cl_2): ν_{CO}, 2027 s, 1992 w, 1800 w, 1743 s cm^{-1}. Following a procedure similar to that for **12**, the reaction of **2** and **3** with phen in the presence of $NaPF_6$ gave only one identical product $[Ru_2(\mu\text{-Pz}')(\mu\text{-CO})_2(CO)_2(\mu_1,\eta^2\text{-phen})_2][PF_6]$ (**15**) in 78 and 80% yield, respectively. Anal. Calcd for $C_{33}H_{23}F_6N_6O_4PRu_2$: C, 43.33; H, 2.53; N, 9.18. Found: C, 43.28; H, 2.60; N, 9.37. ^1H NMR (25 °C, 200 MHz, $CDCl_3$): phen at 10.65 (d, 4 H, J = 5.2), 9.20 (d, 4 H, J = 8.2), 8.62 (dd, 4 H, J = 5.2, 8.2), 8.54 (s, 4 H); H^4 on μ-Pz′ at 4.78 (s, 1 H); Me^3 and Me^5 on μ-Pz′ at 2.81 (s, 6 H). IR (CH_2Cl_2): ν_{CO}, 2026 s, 1991 w, 1801 w, 1744 s cm^{-1}.

Reaction between $Et_3O^+BF_4^-$ and 1−3. A typical reaction is shown as follows. To the solution of **1**, prepared by dissolving **1** (100 mg, 0.171 mmol) in 1 mL of MeCN and 10 mL of CH_2Cl_2 in a 100-mL Schlenk flask, was added with 1 mL of $Et_3O^+BF_4^-$ solution (1 M in CH_2Cl_2). The mixture was then stirred for 1 h at room temperature, giving a solution IR spectrum with three typical carbonyl stretching bands at 2062 m, 2033 s, and 1993 s cm^{-1} for $[Ru_2(CO)_4(MeCN)_6][BF_4]_2$,[4] which can be converted into $[Ru_2(CO)_4(MeCN)_4(PPh_3)_2][BF_4]_2$ by following the established procedure.[4a] Yield: 90%.

Reaction between $Et_3O^+BF_4^-$ and 4−6. A typical reaction is shown as follows. To the solution of **4**, prepared by dissolving **5** (100 mg, 0.101 mmol) in 10 mL of CH_2Cl_2 and 1 mL of MeCN in a 100-mL Schlenk flask, was added with 0.5 mL of $Et_3O^+BF_4^-$ solution (1 M in CH_2Cl_2). The mixture was then stirred for 2 h at room temperature, and 5 mL of MeOH was added to decompose unreacted $Et_3O^+BF_4^-$. Volatile substance was removed under vacuum. Recrystallization from CH_2Cl_2/MeOH gave 105 mg of pure solid. It was identified as $[Ru_2(CO)_4(MeCN)_4(PPh_3)_2][BF_4]_2$ by comparing the spectral evidences with those reported.[4] Yield: 88%.

Reaction between 4 and I_2. In a 100-mL Schlenk flask was added **4** (107 mg, 0.110 mmol) and 5 mL of CH_2Cl_2 at room temperature. This solution was then added dropwise with a CH_2Cl_2 solution of I_2, prepared by dissolving 2 equiv of I_2 (ca. 0.060 g) in 5 mL of CH_2Cl_2. The mixture was stirred for 0.5 h, and the solvent was then removed under vacuum. Recrystallization from CH_2Cl_2/MeOH afforded 0.108 g of the pure product $[Ru_2(\mu\text{-Pz})_2(\mu\text{-I})(CO)_4(PPh_3)_2][I_3]$ (**16**) in 73% yield. Anal. Calcd for $C_{46}H_{36}I_4N_4O_4P_2Ru_2$: C, 37.32; H, 2.45; N, 3.78. Found: C, 37.56; H, 2.54; N, 3.92. ^1H NMR (25 °C, 200 MHz, acetone-d_6): PPh_3 at 7.79−7.53 (m, 30 H); H^3 and H^5 on μ-Pz at 6.99 (d, 4 H, J = 2.3); H^4 on μ-Pz at 5.74 (t, 2 H). $^{31}P\{^1H\}$ NMR (25 °C, 162 MHz, acetone-d_6): 38.74 (s, 2 P). IR: ν_{CO}, 2072 s, 2024 s cm^{-1} in CH_2Cl_2; ν_{CO}, 2068 s, 2016 s cm^{-1} in KBr.

Single-Crystal X-ray Diffraction Studies of 2, 5, 10−12, and 14−16. Suitable single crystals were grown from CH_2Cl_2/hexane or CH_2Cl_2/Et_2O at room temperature to do the single-crystal structure determination. The X-ray diffraction data for **2**, **5**, **10**, and **16** were measured on a four-circle diffractometer, and those for **11**, **12**, **14**, and **15** were measured in frames with increasing ω (0.3°/frame) and with the scan speed at 10.00 s/frame on a Siemens SMART-CCD instrument, equipped with a normal focus and 3 kW sealed-tube X-ray source. For data collected on the four-circle diffractometer, three standard reflections were monitored every 1 h or every 50 reflections throughout the collection. The variation was less than 2%. Empirical absorption corrections were carried out on the basis of an azimuthal scan. For **2**, the structure was solved by direct methods and refined by a full-matrix least-squares procedure using TEXSAN.[8] For **5** and **10**, the structures were solved by heavy-atom method and refined by a full-matrix least-squares procedure using NRCVAX.[9] For **11**, **12**, and **14**−**16**, the structures were solved by direct methods and refined by a full-matrix least-squares procedure using SHELXTL-PLUS.[10] The other essential details of single-crystal data measurement and refinement are given in Table 2. One molecule of CH_2Cl_2 was found in the asymmetric unit of the crystals used for **11**, **12**, and **14**, whereas one and a half molecules of CH_2Cl_2 were located for **16**. The solvent hydrogen positions in this structure were not included in the structure refinement.

Acknowledgment. Financial support for this work by the National Science Council of Republic of China (Contract NSC85-2113-M006-012) is gratefully acknowledged.

Supporting Information Available: An ORTEP plot for **14B** (Figure 9) and tables of non-hydrogen atomic coordinates and equivalent isotropic displacement coefficients, complete bond lengths and angles, anisotropic displacement coefficients, and hydrogen coordinates and B values for **2, 5, 10**−**12**, and **14**−**16** (58 pages). Ordering information is given on any current masthead page.

OM9600708

(8) Crystal Structure Analysis Package, Molecular Structure Corp., The Woodlands, TX, 1985, 1992.
(9) Gabe, E. J.; Le page, Y.; Charland, J.-P.; Lee, F. L.; White, P. S. *J. Appl. Crystallogr.* **1989**, *22*, 384.
(10) (a) Sheldrick, G. M. *SHELXTL-Plus Crystallographic System*, release 4.21; Siemens Analytical X-ray Instruments: Madison, WI, 1991. (b) Siemens Analytical X-ray Instruments Inc., Karlsruhe, Germany, 1991.